# Application of a multiphase CFD modelling approach to improve ozone residual monitoring and tracer testing strategies for full-scale drinking water ozone disinfection processes

Jianping Zhang, Peter M. Huck, Gordon D. Stubley and William B. Anderson

## ABSTRACT

A multiphase computational fluid dynamics (CFD) model has been developed to address the major components of ozone disinfection processes: contactor hydraulics, ozone decay and mass transfer. The model was applied to simulate ozone profiles and tracer residence time distributions of ozone contactors at the DesBaillets Water Treatment Plant (WTP) in Montréal, Canada. The modelling results showed that ozone residuals at the cross-section of the outlet of each chamber in the ozone contactors were very sensitive to monitoring point selection. The optimum locations were significantly affected by multiple operational parameters including water/gas flow rates, ozone dosage and baffling conditions. The modelling results suggested that multiple monitoring points should be used to obtain more representative ozone residuals. The CFD model was also used to study the factors affecting tracer residence time distribution (RTD). It was observed that the method of tracer injection could slightly affect tracer RTD results while sampling location had a significant influence on tracer RTD prediction or measurement. Therefore, it is suggested that multiple sampling points should be employed during tracer tests if possible.

**Key words** | computational fluid dynamics, disinfection, ozonation, ozone residual monitoring, tracer testing strategies

**Jianping Zhang**
**Peter M. Huck** (corresponding author)
**William B. Anderson**
Department of Civil and Environmental Engineering,
University of Waterloo, ON,
Canada N2L 3G1
Tel.: 519 888 4567 Ext. 32707
Fax: 519 746 7499
E-mail: *pm2huck@civmail.uwaterloo.ca*

**Gordon D. Stubley**
Department of Mechanical and Mechatronics Engineering,
University of Waterloo, Waterloo, ON,
Canada N2L 3G1

## INTRODUCTION

The USEPA Surface Water Treatment Rule (SWTR) Guidance Manual (USEPA 1991) recommended that the microbial inactivation credit of an ozone contactor can be evaluated by a 'CT' concept, which is defined as the product of ozone concentration ('C') in a chamber and disinfectant contact time or exposure time ('T'). Depending on the configuration of ozone contactors, CT values can be calculated by $CT_{10}$, completely stirred tank reactor (CSTR), or extended CSTR methods (USEPA 2006). The $CT_{10}$ method is most commonly used by water suppliers despite the fact that, in most cases, it underestimates disinfection efficiency (Rakness 2005). In this method, C is the effluent disinfectant residual of a chamber and $T_{10}$ is the detection time corresponding to the time for which 90% of the water has been in contact with at least the residual concentration, C (USEPA 1991).

CT tables relating *Giardia* and virus log inactivations with associated ozone CT values were given in the SWTR Guidance Manual (USEPA 1991). In the recently released Long Term 2 Enhanced Surface Water Treatment Rule (LT2ESWTR), an additional CT table was provided to calculate the log inactivation rate of *Cryptosporidium parvum* by ozone (USEPA 2006). Depending on temperature, *Cryptosporidium* CT values are 15 to 25 times higher than CT values for equivalent *Giardia* and virus log-inactivation credit. Similar CT tables have been adopted

doi: 10.2166/aqua.2008.038

by some Canadian provincial regulations such as the Procedure for Disinfection of Drinking Water in Ontario (MOE 2006). The direct effect of this new CT table is that the ozone dose needed for *Cryptosporidium parvum* inactivation will be much greater than the dose for *Giardia* and virus inactivation. Therefore, to reduce operational costs and disinfection by-product formation associated with this increase in ozone dose, water suppliers have to accurately determine CT values.

The ozone residual value, C, can be obtained from on-line ozone residual analysers or measured from grab samples (USEPA 2006). Accurate ozone residual data will allow the calculation of correct log-inactivation values and allow optimized performance to be maintained. However, based on reported pilot and full-scale studies, the ozone residual profile in a contactor may vary significantly depending on the method of operation, water quality and water flow conditions (Bellamy 1995; Chen 1998). The potential variation of ozone concentration at sampling locations may greatly affect the ozone concentration monitoring results. One way to determine the optimal sampling locations is through numerical modelling. However, to date no modelling studies have been reported to determine the variation of ozone residuals in ozone contactors with respect to the optimization of ozone residual monitoring strategies.

The disinfectant contact time, $T_{10}$, is usually determined by conducting step or pulse input tracer studies. Teefy (1996) proposed general guidelines for performing tracer tests at water treatment facilities. However, since what occurs within an ozone contactor is a multiphase process, the flow pattern within the contactor is more complex. Therefore, the accuracy of tracer test results can be more strongly affected by factors including the stability of the water/gas flow, tracer injection location, sampling location and tracer detection method. In addition, tracer testing for an ozone contactor system is costly and time-consuming. Thus, there is also a need to optimize tracer test strategies to be used for accurate determination of ozone contactor hydraulics.

Previously reported studies have concentrated on modelling the hydrodynamics and disinfection performance using reactor theory models, such as completely stirred tank reactor (CSTR), plug flow reactor (PFR), completely stirred tank reactor (CSTR) cascade, axial dispersion reactor, back-flow cell, and various combinations of these models (Roustan *et al.* 1992; Zhou *et al.* 1994; Chen 1998; Kim *et al.* 2002). The advantages of these models are their simplicity and hence ease of solution. However, these models are not capable of predicting detailed, three-dimensional ozone contactor performance. In addition, they rely on empirical inputs, such as axial dispersion coefficients (Chen 1998; Kim *et al.* 2002). These empirical inputs are case dependent and cannot be extrapolated to other geometries, scales and operating conditions (Cockx *et al.* 1997). However, these shortcomings can be overcome by the use of computational fluid dynamics (CFD).

CFD is the science of predicting fluid flow, mass transfer, chemical reactions and related phenomena by solving the mathematic equations governing these processes using numerical algorithms (Versteeg & Malalasekera 2002). CFD has come into use recently for evaluating ozone disinfection systems (Murrer *et al.* 1995; Do-Quang *et al.* 1999; Ta & Hague 2004). These models are developed for either homogeneous or heterogeneous flow regimes. They provide a good platform for estimation of non-ideal flow behaviours of the fluid phases. In our earlier publication (Zhang *et al.* 2005), we validated a three-dimensional multiphase CFD model based on full-scale ozone contactor studies and applied the model to predict disinfection performance. To the best of our knowledge, the optimization of ozone residual monitoring and tracer test methods has not been reported in the literature.

The primary objective of the work reported in this paper was to apply a computational fluid dynamics (CFD) modelling approach to investigate the ozone concentration variation at outlets of ozone chambers and to optimize the locations of ozone residual monitoring points. The second objective was to study the effects of tracer injection methods and tracer monitoring points on tracer test results with respect to optimizing tracer test strategy.

## NUMERICAL METHODS

### Modelling of contactor hydrodynamics

In this study, two phases were defined for modelling of ozonation processes: the continuous phase (water) and the

dispersed phase (ozonated gas). The Eulerian–Eulerian approach was used for simulating bubbles dispersed in water during ozonation processes. Each phase was treated as an interpenetrating continuum and the volume fraction of a phase represents the fraction of the control volume that is occupied by this phase (Lakehal 2002; Versteeg & Malalasekera 2002; Zhang 2007). The hydrodynamic CFD model was based on continuity and momentum balance equations for the two phases (gas and liquid). The general CFD model for multiphase problems includes the following conservation Equations (Versteeg & Malalasekera 2002; Michele 2002):

$$\frac{\partial}{\partial t}(\rho_\alpha r_\alpha) + \frac{\partial}{\partial x_i}(\rho_\alpha r_\alpha u_{\alpha,i}) = 0 \tag{1}$$

$$\frac{\partial}{\partial t}(\rho_\alpha r_\alpha u_{\alpha,i}) + \frac{\partial}{\partial x_j}(\rho_\alpha r_\alpha u_{\alpha,i} u_{\alpha,j}) = -r_\alpha \frac{\partial p_\alpha}{\partial x_i} + \frac{\partial}{\partial x_i} r_\alpha \mu_\alpha \left(\frac{\partial u_{\alpha,i}}{\partial x_j} + \frac{\partial u_{\alpha,j}}{\partial x_i}\right) + M_{\alpha,i} \tag{2}$$

$$\sum_{\alpha=1}^{N_p} r_\alpha = 1 \tag{3}$$

where, $\rho_\alpha$ is the material density of the $\alpha$ phase (gas or liquid phase); $r_\alpha$ is the volume fraction of the $\alpha$ phase; $u_{\alpha,j}$ is the flow velocity of the $\alpha$ phase in the $i$-direction; subscript $j$ refers to the $j$ direction; $M_{\alpha,i}$ describes the interfacial forces acting on phase $\alpha$ due to the presence of other phases. The total interfacial force acting between two phases may arise from several independent physical effects. In the present model, only the interphase drag force and turbulence dispersion force were considered, because the effects of other non-drag forces become less significant in large gas–liquid phase columns (Lo 2000; Vesvikar & Al-Dahhan 2005).

The interphase drag force, $M^D_{\alpha\beta}$, was modelled with the Grace Drag model (Clift *et al.* 1978), which was developed using air–water data (Vesvikar & Al-Dahhan 2005). The model was chosen for this study since ozone disinfection processes consist mainly of air and water phases. The Grace Drag model is expressed as:

$$M^D_{g,l} = \frac{3}{4}\rho_l \frac{r_g}{d_g} C_D (u_g - u_l)|u_g - u_l| \tag{4}$$

where, $d_g$ is the gas bubble diameter, $u_g$ and $u_i$ are the gas and liquid velocities, and $C_D$ is the drag coefficient (Lo 2000).

The turbulent dispersion force, $M^{TD}_{\alpha\beta}$, considers the additional dispersion of phases from high volume fraction regions to low volume fraction regions due to turbulent fluctuations. The model of Lopez de Bertodano (1991) was used in this study for describing the turbulent dispersion force:

$$M^{TD}_l = M^{TD}_g = -c_{TD}\rho_l k_l \nabla r_l \tag{5}$$

where $c_{TD}$ is the dispersion coefficient, for which values of 0.1–0.5 have been used successfully for bubbly flow with bubble diameters in the order of a few millimetres. The dispersion coefficient was taken as 0.1 in this study, which is suitable for the bubble size range utilized (Gobby 2004); $k_l$ is the turbulent kinetic energy of the liquid phase which is described below.

The impact of turbulence on ozone contactor hydrodynamics was modelled in both gas and liquid phases. For the liquid phase, the standard k–$\epsilon$ model was used (Launder & Spalding 1974), because at this point in time the $k$–$\epsilon$ model is the most commonly used turbulence model for solving engineering CFD problems (Schugerl & Bellgardt 2001; Michele 2002). The turbulence of the dispersed gas phase was modelled using a dispersed phase zero equation model and bubble induced turbulence was taken into account according to Sato & Sekoguchi (1975).

## Modelling of ozone mass transfer and reactions

Ozone must be dissolved from the gas to the liquid phase before reacting with contaminants (including pathogens) in water. The following species transport equations were solved for ozone mass transfer and reactions:

$$\frac{\partial}{\partial t}(r_\alpha \rho_\alpha \phi_\alpha) + \nabla\cdot(r_\alpha U_\alpha \rho_\alpha \phi_\alpha) - \nabla\left(r_\alpha\left(\rho_\alpha D^{(\phi)}_\alpha + \frac{\mu_{t\alpha}}{Sc_{t\alpha}}\right)\nabla\phi_\alpha\right) = S^{(\Phi)}_\alpha \tag{6}$$

where $r_\alpha$ is the volume fraction of each phase; $U_\alpha$ is the flow velocity; $\rho_\alpha$ is the density of phase $\alpha$; $\phi_\alpha$ is the conserved quantity per unit mass of phase $\alpha$; $D^{(\phi)}_\alpha$ is the kinematic diffusivity for the scalar in phase $\alpha$; $Sc_{t\alpha}$ is the turbulent

Schmidt number; $S_\alpha^{(\Phi)}$ is the volumetric source term, which is determined by the mass transfer rate and/or reaction rate.

The interfacial mass transfer of ozone between the gas and the water can be modelled based on the well-known two film theory (Danckwerts 1970; Singer & Hull 2000), and the source term for this transferring process can be expressed as:

$$S_{\mathrm{tr}} = k_{\mathrm{l,tr}} a [C_{\mathrm{l}}^{*} - C_{\mathrm{l}}] \tag{7}$$

$$a = \frac{6}{d_g} * r_g \tag{8}$$

where the source term $S_{\mathrm{tr}}$ represents the rate of interfacial ozone mass transfer between the two phases; $C_{\mathrm{l}}^{*}$ is the saturation concentration of ozone in water; $C_l$ is the local ozone residual concentration; $k_{l,tr}$ is the liquid phase mass transfer coefficient and was chosen as $5 \times 10^{-4}$ m s$^{-1}$ (Beltran 2004); $a$ is the volumetric interfacial area (1 m$^{-1}$); $r_g$ is the local gas phase fraction; and $d_g$ is bubble diameter. To simplify the model, bubble break-up and coalescence were ignored in this study. It was assumed that the bubbles were spherical with a constant bubble diameter of 3 mm (Langlais *et al.* 1991; Zhou *et al.* 1994; Cockx *et al.* 1999).

The saturation concentration of ozone in water $C_{\mathrm{l}}^{*}$ can be calculated according to Henry's law (Singer & Hull 2000):

$$C_{\mathrm{l}}^{*} = \frac{C_g}{\mathrm{H}} \tag{9}$$

where $C_g$ is the ozone concentration in the gas phase. $H$ is the Henry's law constant which was determined based on an empirical equation developed by Marinas *et al.* (1993).

Once dissolved in water, ozone becomes very unstable. Langlais *et al.* (1991) & Kim *et al.* (2002) indicated that the decomposition of ozone involves two stages: the initial ozone rapid-demand period due to the presence of substances that react with ozone through direct free radical reactions (e.g. natural organic matter (NOM)) and the period of moderate decay consumption, in which ozone decays slowly due to reactions with the remaining substances in water.

Previous studies have shown that the fast reactions in the first stage can be described by a second order kinetic model (Lev & Regli 1992; Chen 1998; Kim *et al.* 2002). Therefore, the source term corresponding to the reactions of this stage was modelled by:

$$S_{\mathrm{demand}} = -k_{\mathrm{NOM_f}} [\mathrm{NOM_f}] C_{\mathrm{l}} \tag{10}$$

in which source term $S_{\mathrm{demand}}$ represents the ozone consumption rate during the first stage which equals the reaction rate of [NOM$_{\mathrm{f}}$]; [NOM$_{\mathrm{f}}$] is the concentration of fast reacting natural organic matter, in units of [kg[$O_3$] m$^{-3}$]; $k_{\mathrm{NOM_f}}$ is a second-order rate constant (m$^3$ kg$^{-1}$ s).

Since the reaction of NOM and ozone is so fast, measurement of $k_{\mathrm{NOM_f}}$ is often difficult (Kim *et al.* 2002). For modelling purposes, the reaction rate $k_{\mathrm{NOM_f}}$ used in this study was set at 3.20 (l mg$^{-1}$ s), based on a study by Hunt & Marinas (1999). This rate constant value was acceptable for modelling purposes because it resulted in more than 90% completion of the second-order reaction in seconds, which is consistent with the experimental observations in this study and previous studies by others (Hunt & Marinas 1999; Kim *et al.* 2002; Tang *et al.* 2005).

The second stage ozone decomposition was described by a pseudo first-order kinetic equation as follows (Langlais *et al.* 1991):

$$S_{\mathrm{decay}} = -\frac{\mathrm{d}C_{\mathrm{l}}}{\mathrm{d}t} = k_{\mathrm{d}} C_{\mathrm{l}} \tag{11}$$

where $S_{\mathrm{decay}}$ is the source term for the decay process, and $k_{\mathrm{d}}$ is the water quality-dependent decay rate constant determined by lab-scale experiments.

## Modelling of tracer residence time distribution

Ozone contactor hydraulic performance can be assessed from tracer residence time distribution (RTD) curves. Step or pulse additions of a tracer can be made resulting in so-called F and E RTD curves (Levenspiel 1999). In this study, numerical simulation of tracer tests was conducted in two steps. First, the steady state fluid flow was established. Second, the steady state flow field solution was applied as an initial condition. A tracer was introduced at a source point in the inlet to the tank, and the concentration at the outlet was tracked by solving the transient tracer scalar transport equation. Simulations with both step and pulse injections were produced. $T_{10}$ values were then obtained from the tracer F curve directly as described by Teefy (1996).

## CASE STUDY

The CFD model was applied to simulate the ozone disinfection system at the 1,200 million litres per day DesBaillets Water Treatment Plant (WTP) in Montreal, Canada. The DesBaillets WTP has six parallel ozone contactors, and each contactor has two cells. Ozone gas is fed in the first cell of each contactor through 126 porous fine bubble diffusers. The total length, width, and height of each contactor are 23.8 m, 5.50 m and 7.16 m, respectively. Figure 1 shows the ozone residual monitoring points inside a DesBaillets ozone contactor. The system initially used two sampling points for measuring ozone residuals: C1 for cell 1 and C2 for cell 2. To improve the accuracy of ozone residual monitoring in cell 1, five additional sampling ports (P1 to P5) were installed. All the sampling ports are located at the middle vertical plane in the contactor. The average ozone residual from these five monitoring points was used for CT calculation instead of using the residual at a single point C1 (Barbeau *et al.* 2003). Teflon tubes were connected to each sampling point on the ozone contactor and valves were used to regulate flows at $3\,l\,min^{-1}$. The flows were directed to 250 − ml glass beakers which overflowed to a drain. Duplicate samples were collected from the beakers using a syringe and slowly injected into the indigo reagent for ozone residual determination (*Standard Methods* 1998; Method 4500-O3, B). This sampling method showed good reproducibility and the average percentage error calculated based on two-duplicated measurements was 3.3% (El-Baz 2002). The contactor hydraulics were evaluated using a step injection of hydrofluorosilic acid as the tracer chemical. A distribution pipe was installed on the inlet surface to provide uniform injection of the tracer chemicals across the width of the contactor during tracer tests. The tracer samples were taken at multiple locations including points P5 and C2, as shown in Figure 1, using Teflon tubes. Forty samples were collected at each sampling point to capture the complete tracer curve. The tracer concentration was measured colorimetrically as described in Standard Methods (Method 4500-F-.D; *Standard Methods* 1998). All the field tests were performed by the École Polytechnique de Montréal (El-Baz 2002; Barbeau *et al.* 2003).

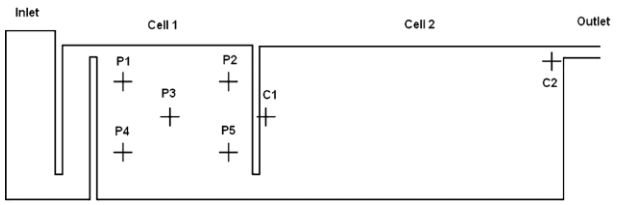


**Figure 1** | Ozone residual sampling ports in a DesBaillets WTP ozone contactor.

The three-dimensional CFD modelling was carried out with a finite-volume based program CFX10 (Ansys 2005). Since the DesBaillets WTP ozone contactor has a symmetric structure, only half of the contactor was modelled to reduce the number of meshes and computational time. Unstructured tetrahedral grids were used for the CFD modelling. A mesh sensitivity study was performed and the total element number was determined to be to 424,891. Further reduction of mesh size did not significantly improve the accuracy of the modelling. The result of the mesh sensitivity study is shown in Appendix 1. As described above, the $k-\epsilon$ model was used to account for the turbulence in the main flow. A comparison of the $k-\epsilon$ model and other commonly used turbulence models is presented in Appendix 2. The results suggested that the $k-\epsilon$ model was appropriate for the study undertaken here.

The boundary conditions of the water and gas inlets were provided by specifying uniform velocities calculated from water and gas flow rates. The water inlet flow rates were in the range of 1.37 to $3.22\,m^3\,s^{-1}$ and the volume fraction of water was 1. The gas inlet flow rates varied from 0.15 to $0.21\,m^3\,s^{-1}$ and the volume fraction of air was 1. The turbulence intensity was set to be 5% based on the Reynolds number and the geometry of the inlet. The outlet was set as a zero pressure gradient boundary condition and the reference pressure was set as 0 atmosphere (atm). The free water surface was set as a degassing outlet which assumed that the surface was flat, frictionless and impervious to liquid to simplify the simulation; however, gas was allowed to leave at the rate at which it arrived at the surface.

The reaction rate $k_{IOD}$ was set at 3.20 ($l\,mg^{-1}\,s$), based on a study by Hunt & Marinas (1999). The ozone demand and decay kinetic constants for the DesBaillets Water Treatment Plant ozone contactor were based on an experimental study performed by the École Polytechnique de Montréal (El-Baz 2002; Barbeau *et al.* 2003). Depending on the water quality and operational parameters, the immediate ozone demand of the source water varies from

0.4 to 1.2 mg l$^{-1}$ and the ozone decay kinetic constant $k_d$ varies in the range of 0.05 to 0.15 min$^{-1}$ (El-Baz 2002).

A second order high-resolution differencing scheme was applied to all flow equations. The time step used varied in range between 100 s and 0.001 s from the start to the end of a run. Three convergence criteria were adopted simultaneously to check the convergence of the numerical solution. The first was the normalized residuals, which were set as 0.0001. The second criterion was the mass imbalances of the fluid domain, which were controlled to be less than 0.1%. The third was to create some monitoring points in the domain and use the values of some key global quantities (e.g. gas holdup) at these points as indicators of convergence. For tracer test simulation, each case was run until tracer mass recovery was greater than 98%. All the simulations were done on a Pentium 4 PC with 3.0 GHz CPU and 2G memory. The computational times for obtaining the converged solutions were usually 1 day to 4 days.

## RESULTS AND DISCUSSION

### Model validation

The CFD model was validated by comparison of the simulated tracer residence time distribution (RTD) with field tracer test data (El-Baz 2002; Barbeau *et al.* 2003) obtained at the DesBaillets WTP ozone disinfection system. Figure 2 presents a comparison of results at a flow rate of 2.16 m$^3$ s$^{-1}$ for monitoring points P5 and C2. The locations P5 and C2 are shown in Figure 1. It can be observed that the CFD simulated tracer RTD curves closely match the experimental tracer test results. The simulated and measured $T_{10}/T_{50}$ ratios at P5 were 0.47 and 0.43, respectively; and the simulated and measured $T_{10}/T_{50}$ ratios at C2 were 0.59 and 0.63, respectively. The differences are less than 11%. These comparison results suggest that CFD modelling can provide reasonable accuracy in predicting ozone contactor hydraulic performance.

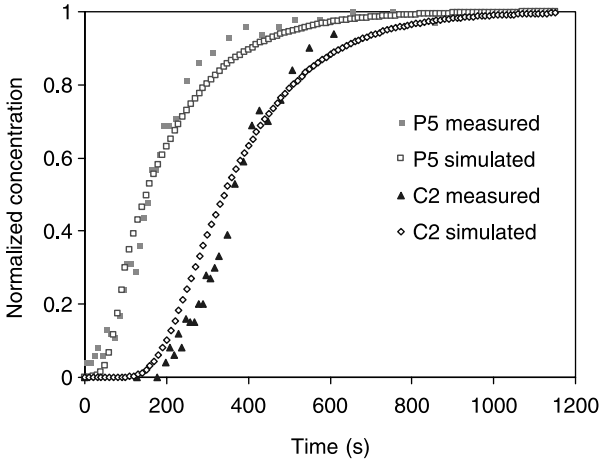


**Figure 2** | Comparison of simulated and experimental tracer curves.

In addition, local ozone residual concentrations were obtained by solving transport equations for ozone mass transfer and reactions. The ozone demand and decay kinetic parameters used were determined by experimental study conducted by the École Polytechnique de Montréal (El-Baz 2002; Barbeau *et al.* 2006). Table 1 presents the comparison between the numerical and measured ozone residual distribution at six monitoring points inside the ozone contactor as shown in Figure 1. The modelling conditions include: water flow rate $= 2.16\,m^3\,s^{-1}$, gas flow rate $= 0.25\,m^3\,s^{-1}$, ozone concentration in gas $= 1.4\%$, immediate ozone demand (IOD) $= 0.96\,mg\,l^{-1}$ and ozone first order decay constant $= 0.12\,l\,min^{-1}$. Though relatively large differences were observed at points P2 and P4, the predicted ozone concentrations at all other monitoring points were within 11% of the measured values. One possible reason for the large variations between the numerical results and experimental measurements at points 2 and 4 is that these two points are located at areas with strong dynamics flows and high ozone gradients: point P4 is near the gas diffusers and point P2 is between the short-circuiting and recirculation zones. The variations may also be caused by uncertainty in some factors in the model (e.g. inlet boundary conditions, bubble break-up and coalescence, numerical description method) (Peplinski & Ducoste 2002; Buwa & Ranade 2002) and experimental errors during field ozone measurement (Rakness 2005).

**Table 1** | Comparison between the predicted and measured ozone concentrations at six monitoring points

| | Monitoring point | | | | | |
|---|---|---|---|---|---|---|
| | P1 | P2 | P3 | P4 | P5 | C2(Outlet) |
| Predicted ozone concentration (mg l$^{-1}$) | 0.60 | 0.34 | 0.81 | 0.76 | 0.71 | 0.64 |
| Measured ozone concentration (mg l$^{-1}$) | 0.54 | 0.44 | 0.74 | 1.03 | 0.64 | 0.67 |
| Difference (%) | 11 | 25 | 10 | 26 | 11 | 5 |

It should be noted that, in the present research, the experimental and CFD predicted ozone residuals were only compared at the existing six monitoring points due to the limitation of the full-scale work. In future work, the spatial ozone residual distribution could be measured in the DesBaillet ozone contactor or full-scale ozone contactors in other treatment plants. Thus a more comprehensive validation could be performed to obtain greater confidence in the CFD modelling approach.

## Distribution of dissolved ozone concentration at the outlet of the cells

When the effluent CT method is used for microbial inactivation credit calculation, the dissolved ozone concentration should be measured at the outlet of each cell (USEPA 1991). However, current regulations do not provide clear guidance on how to locate these ozone monitoring points. It is therefore important to investigate the sensitivity of the sensor locations on ozone residual monitoring to assist with ozone contactor design and operation.

Figure 3 presents the CFD simulated ozone profiles at different planes at the outlet area of cell 1. As shown in Figure 3, the Y axis represents distance along the width of the contactor from the central symmetric plane and the X axis represents vertical distance from the bottom of the contactor. It can be observed that the ozone concentration varied widely at the outlet, which is caused by strong turbulence and the existence of short-circuiting in this area. The residuals were above 1.0 mg $l^{-1}$ at the centre area of the outlet planes and decreased to 0.2 mg $l^{-1}$ at the locations close to the side walls. The maximum value could be more than five times higher than the minimum value. The modelling results also indicated that ozone residuals were more sensitive to the sampling locations at the outlet area of cell 1. Measuring ozone residual upstream or downstream of the baffle may lead to under- or over-estimation of outlet ozone concentrations. Under the current regulatory framework (MENV 2002; USEPA 2006), C represents the outlet concentration of a cell. Therefore, the present work suggests that the ozone sensor or sampling port should be located within the plane under the baffle wall.

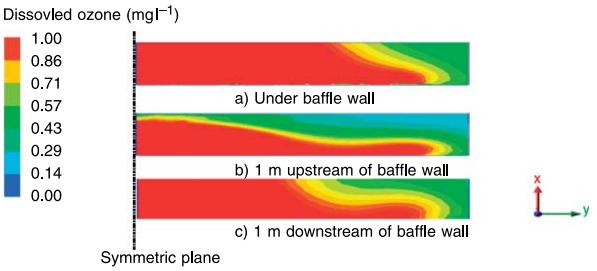


**Figure 3** | Simulated ozone residual distributions around the outlet of cell 1 in the DesBaillets WTP ozone contactor (only half of the outlet is shown).

Based on the drinking water regulations of the province of Quebec, Canada (MENV 2002), the CT value of the first cell is calculated based on the residence time $T_{10}$ of the cell multiplied by half of the ozone residual at the outlet of the cell. The above result indicated that the selection of inappropriate monitoring points would lead to incorrect calculation of CT values for log inactivation evaluation. This conclusion may be applied to ozone contactors with multiple ozone diffusing chambers; in these contactors, ozone concentration could vary significantly at the outlets of these chambers.

Using this CFD modelling approach, it is possible to locate the potential 'optimal' location for ozone residual monitoring under a specific operational condition. The shaded region in Figure 4 shows the area at the outlet of a cell where calculated ozone concentrations were within ±20% of the average outlet ozone concentration calculated through CFD modelling. The 20% value was chosen as a reasonable one for illustration purposes.

It would be expected that more representative monitoring results could be obtained when ozone sampling ports or online sensors were installed within or close to the shaded area shown in Figure 4. However, the ozone residual distributions at the outlet of cell 1 were strongly affected by the operational parameters.

Figure 5 shows the variation of the 'optimal' ozone sampling zones at two different water and air flow rates.


**Figure 4** | Area at the outlet of cell 1 where ozone concentrations are within ±20% of the average value (water flow rate = 3.22 $m^3 s^{-1}$; gas flow rate = 0.21 $m^3 s^{-1}$; ozone dose = 2.2 mg $l^{-1}$).

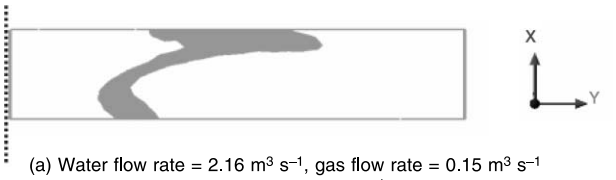


(a) Water flow rate = 2.16 $m^3 s^{-1}$, gas flow rate = 0.15 $m^3 s^{-1}$ ozone dose = 2.0 $mg l^{-1}$


(b) Water flow rate = 1.37 $m^3 s^{-1}$, gas flow rate = 0.18 $m^3 s^{-1}$ ozone dose = 2.0 $mg l^{-1}$

**Figure 5** | Area at the outlet of cell 1 where ozone concentrations are within ±20% of the average value.

Since the shape of the optimal zones changed significantly at different conditions, it would be difficult to determine a universal optimal point which could always represent the average ozone residual.

Previous studies have shown that other factors, such as ozone dosage and water quality, might also affect the dissolved ozone concentration distribution (Bellamy 1995). It is therefore suggested that multiple ozone monitoring points should be provided at the outlet of cell 1 to obtain a more representative ozone residual, if possible.

Figure 6 shows an example of three monitoring points (S1 to S3) evenly distributed across half of the cell 1 outlet. Table 2 presents a comparison of the mass flow averaged ozone concentration, residual at point C1 (shown in Figure 1), and the average ozone residual calculated from the three points. It can be seen that the residuals at point C1 were higher than the outlet average residuals at the current modelling conditions. The three point averaged ozone residual was in reasonable agreement with the averaged residual at the outlet of cell 1. Using this multiple points monitoring strategy, a more representative ozone residual for the cell 1 outlet concentrations can be obtained.

## Spatial distribution of dissolved ozone concentration within ozone contactors

The DesBaillets WTP initially used point C1 (see Figure 1) as the ozone residual monitoring point to calculate the CT of cell 1. This monitoring point is located just downstream of the baffle wall and in the region of short-circuiting caused by buoyancy flow. Therefore it usually over-estimates the ozone residual in Cell 1, and is not appropriate for use in CT calculations. To improve the accuracy in monitoring ozone residuals, five additional monitoring points have been installed in Cell 1 of the DesBaillets ozone contactor to obtain the average ozone residual in this cell for CT calculation.

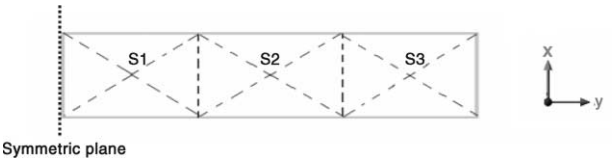


**Figure 6** | Location of three sampling points at the outlet of cell 1.

Figure 7 shows the modelled spatial variation of the ozone residual profile at a water flow rate of 3.25 $m^3 s^{-1}$, gas flow rate of 0.27 $m^3 s^{-1}$, and ozone dosage of 2.20 $mg l^{-1}$. The CFD results indicated that ozone concentrations at the plane closest to the side wall (plane A) were much smaller than those at the other two locations (planes B and C). Therefore installing sampling ports close to, or flush with, the walls should be avoided to prevent under-estimation of average ozone concentration. It can also be observed that the dissolved ozone concentrations varied significantly along the length of the contactor which was attributed to the existence of short-circuiting and recirculation zones within the contactor as shown in Figure 8.

Table 3 shows a comparison of the volume averaged residual and average residual calculated from five points at different planes. The volume averaged residual was calculated as the integral of ozone concentration in cell 1 divided by the total volume of cell 1. It was found that installing the five monitoring points on the middle plane (plane C) might over-estimate the volume averaged ozone residual, while putting monitoring points on the plane closest to the wall (Plane A) may under-estimate ozone residuals. A better prediction of the averaged ozone residual could be obtained by installing the monitoring points on the plane 1.2 m away from the middle plane.

Although the results for the averages of the five points in plane B best predict the volume average, these results are specific to the DesBaillets water treatment plant contactor and are limited to the modelled conditions. Experimental tests would need to be performed to verify these numerical results.

**Table 2** | Comparison of the mass flow averaged ozone concentration and the arithmetic average residual calculated from three points at outlet of cell 1

| | Ozone residual at cell 1 (mg $l^{-1}$) | | |
|---|---|---|---|
| **Modelling conditions** | **Outlet average** | **Residual at point C1** | **Three points (S1 to S3) average*** |
| Water flow rate: 3.22 $m^3 s^{-1}$<br>Gas flow rate: 0.21 $m^3 s^{-1}$<br>Ozone concentration in air: 0.015 kg $m^{-3}$<br>Ozone demand: 0.60 mg $l^{-1}$<br>Ozone decay constant: 0.10 $min^{-1}$ | 1.09 | 1.45 | 1.07 |
| Water flow rate: 2.16 $m^3 s^{-1}$<br>Gas flow rate: 0.15 $m^3 s^{-1}$<br>Ozone concentration in air: 0.0167 kg $m^{-3}$<br>Ozone demand: 0.53 mg $l^{-1}$<br>Ozone decay constant: 0.12 $min^{-1}$ | 0.85 | 1.25 | 0.94 |
| Water flow rate: 1.37 $m^3 s^{-1}$<br>Gas flow rate: 0.18 $m^3 s^{-1}$<br>Ozone concentration in air: 0.016 kg $m^{-3}$<br>Ozone demand: 0.69 mg $l^{-1}$<br>Ozone decay constant: 0.10 $min^{-1}$ | 0.98 | 1.01 | 0.97 |

*Arithmetic average.

## Effects of tracer injection points on RTD and $T_{10}$

The ozone contactor hydraulics, represented by residence time distribution (RTD) or $T_{10}$, are usually determined by conducting chemical tracer testing (Teefy 1996). The CFD model was also used to study factors affecting tracer residence time distribution (RTD). Numerical tracer tests were performed by pulse-injecting a predetermined amount of tracer in a very short time (0.2 seconds) from the inlet of the contactor and monitoring the tracer concentration at the outlet of the contactor. Figure 9 shows the simulated tracer residence time distribution curves (E curves) obtained through four different tracer injections:

1. 'Tracer 1' was injected at an inlet point close to the side wall
2. 'Tracer 2' was injected at an inlet point between the side wall and middle symmetric plane
3. 'Tracer 3' was injected at an inlet point on the middle symmetric plane
4. 'Tracer inlet' was injected uniformly over the cross-section of the contactor inlet

These tracer curves were generated at a water flow rate of 3.25 $m^3 s^{-1}$, gas flow rate of 0.27 $m^3 s^{-1}$ and ozone dosage

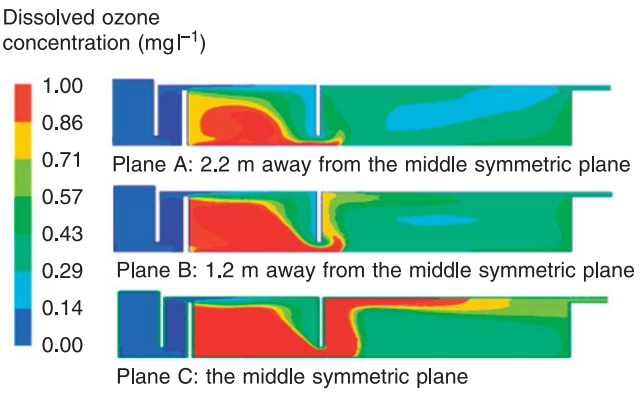


**Figure 7** | Spatial ozone residual distributions along the horizontal profile of the DesBaillets WTP ozone contactor.

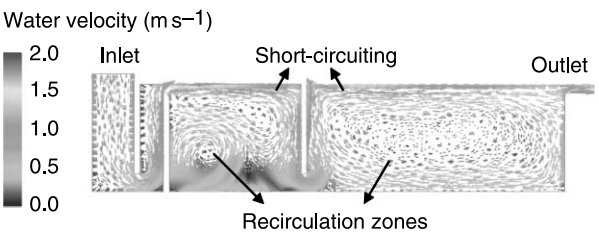


**Figure 8** | Typical velocity field in the DesBaillets WTP ozone contactor.

**Table 3** | Comparison of the volume averaged residual and arithmetic average residuals calculated from five points at different planes

| | Ozone residual at cell 1 (mg $l^{-1}$) | | | |
|---|---|---|---|---|
| **Modelling conditions** | **Volume average** | **5 points average* in plane A** | **5 points average* in plane B** | **5 points average* in plane C** |
| Water flow rate: 0.28 $m^3 s^{-1}$<br>Gas flow rate: 0.02 $m^3 s^{-1}$<br>Ozone concentration in air: 0.015 kg $m^{-3}$<br>Ozone demand: 0.60 mg $l^{-1}$<br>Ozone decay constant: 0.10 $min^{-1}$ | 0.99 | 0.69 | 0.93 | 1.27 |
| Water flow rate: 0.186 $m^3 s^{-1}$<br>Gas flow rate: 0.011 $m^3 s^{-1}$<br>Ozone concentration in air: 0.017 kg $m^{-3}$<br>Ozone demand: 0.53 mg $l^{-1}$<br>Ozone decay constant: 0.12 $min^{-1}$ | 0.69 | 0.46 | 0.73 | 0.86 |
| Water flow rate: 0.127 $m^3 s^{-1}$<br>Gas flow rate: 0.013 $m^3 s^{-1}$<br>Ozone concentration in air: 0.016 kg $m^{-3}$<br>Ozone demand: 0.69 mg $l^{-1}$<br>Ozone decay constant: 0.10 $min^{-1}$ | 0.82 | 0.53 | 0.76 | 0.94 |

*Arithmetic average.

of 2.20 mg $l^{-1}$. For this specific case, the tracer injection method only slightly influenced tracer RTDs. Tracer 1 had the highest $T_{10}$ (164 seconds) and Tracer 3 had the lowest $T_{10}$ (155 seconds). Only a very small difference (< 6%) was observed for different injection points, which was probably because the DesBaillets WTP contactor has two small cells before cell 1. These two cells allowed the tracer chemicals to be mixed and more uniformly distributed prior to entering cell 1.

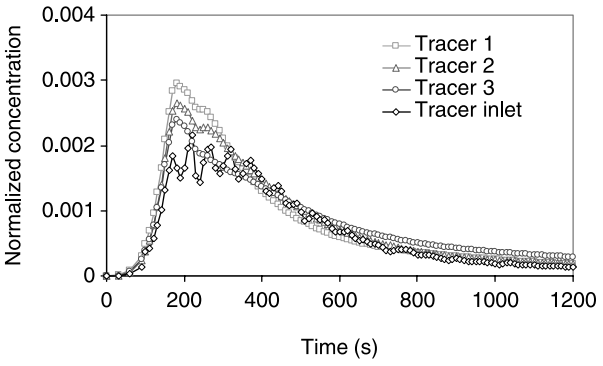


**Figure 9** | Effects of tracer injection location on tracer residence time distribution.

The current simulation results suggest that the injection point does not have a significant influence on the DesBaillets ozone contactor residence time distribution. Additional experimental tests would need to be done to confirm these numerical results. Until such analysis is performed, tracer injections should be made at points upstream from the contactor to ensure that the tracer is well mixed with the entire influent water.

## Effects of tracer monitoring point selection on RTD and $T_{10}$

The effects of tracer monitoring points on tracer RTD tests were also studied. The concentration of chemical tracer was monitored at three points located at the contactor outlet. Point 1 is 0.5 m away from the side wall, point 3 is on the middle symmetric plane and is 2.75 m away from the side

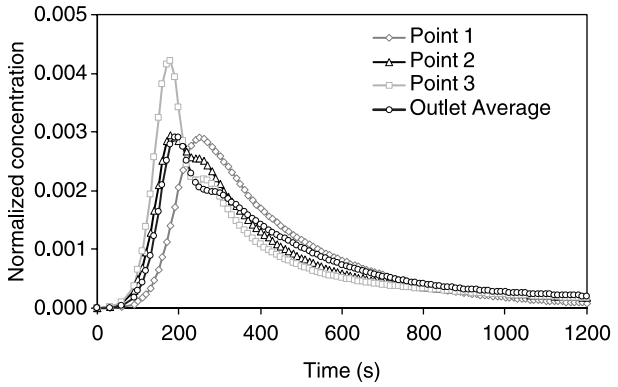


**Figure 10** | Effects of tracer monitoring points on residence time distribution.

wall, and point 2 is located between points 1 and 3. Figure 10 presents the simulated tracer RTD curves for the three points. The RTD curve obtained from the numerical monitoring of average chemical tracer at the contactor outlet is also shown for comparison purposes. Significant differences in the tracer RTDs were observed at the three different tracer monitoring points. The $T_{10}$ calculated from these RTD curves differed by more than 20% ($T_{10}$ values of points 1, 2 and 3 and the outlet average were 145, 160, 172 and 185 seconds, respectively). Since the tracer RTD of monitoring point 2 was close to the average RTD curve, it might be more appropriate for the contactors studied. This result also suggested that more accurate tracer RTD and $T_{10}$ information could be obtained if multiple monitoring points were used and the tracer RTD was calculated by averaging the measured tracer concentrations at different monitoring points.

## CONCLUSIONS

This work evaluated a computational fluid dynamics (CFD) modelling approach for the determination of CT values in a full-scale ozone contactor at the DesBaillets Water Treatment Plant in Montreal, Canada. The important conclusions of this study are the following:

- For the first time, a CFD modelling approach was applied to illustrate and improve an ozone residual monitoring strategy. The modelling results showed that ozone residuals in the cross-section of the outlet of cell 1 in the DesBaillets ozone contactors differed as much as five-fold. The variation of ozone residual concentrations was found to be affected by multiple factors, including water flow rate, gas flow rate, ozone dosage and ozone reaction kinetics. Therefore, it is suggested that multiple ozone residual sampling points should be installed at the outlet of ozone contactor chambers containing or close to bubble diffusers to provide more accurate indicators of the true ozone residuals.
- For the ozone contactor that was modelled, the installation of five monitoring points on the middle plane of cell 1 or on a plane close to the side wall showed that over- or under-estimation of the volume average ozone residual was possible. A better prediction of the volume average residual can be obtained when the monitoring points are installed on a plane located 1.2 m away from middle plane.
- The CFD model was also used to study the factors affecting the residence time distribution (RTD). The results suggested that the selection of tracer injection locations as well as tracer sampling locations could affect the RTD prediction or measurement. The CFD predicted $T_{10}$ values showed that RTD curves at different outlet locations varied by more than 20%. It is therefore recommended that multiple sampling points be employed during tracer tests.
- The CFD modelling results agreed well with full-scale experimental data, including tracer testing results and measured ozone profiles.
- The results of this specific ozone contactor study suggested that a multiple-point sampling strategy is necessary for optimization of ozone residual measurement and tracer testing, and therefore should be considered at the contactor design phase.

It should be noted that, at the moment, the strategies proposed for ozone residual monitoring and tracer testing are specific to the DesBaillets water treatment plant contactor. Further studies should be done in the future to optimize the selection of ozone residual sampling points and to determine the best tracer test method for different types of ozone contactor based on CFD modelling and experimental study. Ultimately, a guideline document could be developed for various basic contactor designs.

## ACKNOWLEDGEMENTS

Funding for this project was provided by the Natural Sciences and Engineering Research Council of Canada (NSERC) in the form of an Industrial Research Chair at the University of Waterloo, and by the Canadian Water Network in the form of a grant (the project was led by École Polytechnique de Montréal). The current Chair partners include: American Water Canada Corp., Brightwell Technologies Inc., the cities of Brantford, Guelph, Hamilton, Ottawa and Toronto, Conestoga-Rovers & Associates Limited, EPCOR Water Services, the Ontario Clean Water Agency (OCWA), PICA USA Inc., RAL Engineering Ltd, the Region of Durham, the Regional Municipalities of Niagara and Waterloo, Stantec Consulting Ltd and GE Zenon (formerly Zenon Environmental Inc). The authors would like to acknowledge the contributions of Dr Benoit Barbeau at École Polytechnique de Montréal for his support with respect to data collection and field investigation of the DesBaillets WTP ozone contactors.

## REFERENCES

ANSYS 2005 *CFX 10 User Manual*. Ansys Inc., www.ansys.com/

Barbeau, B., El-Baz, G., Sarrazin, V. & Desjardins, R. 2003 Application of the integrated disinfection design framework (IDDF) for disinfection contactor performance evaluation. Proceedings of the *American Water Works Association Water Quality Technology Conference (WQTC)*, Philadelphia, Pennsylvania, CD-ROM.

Barbeau, B., Bouchard, C. & Broseus, R. 2006 Validation of full-scale ozone contactor performance using biodosimetry. *Proceedings of the American Water Works Association Water Quality Technology Conference and Exposition (WQTC)*, Denver, Colorado, CD-ROM.

Bellamy, W. D. 1995 *Full-scale Ozone Contactor Study*. Report No 90668, American Water Works Association Research Foundation, Denver, Colorado.

Beltran, F. J. 2004 *Ozone Reaction Kinetics for Water and Wastewater Systems*. Taylor & Francis Group, New York.

Buwa, V. V. & Ranade, V. V. 2002 Dynamics of gas-liquid in a rectangular bubble column: experiments and single/multi-group CFD simulations. *Chem. Eng. Sci.* **57**, 4715–4736.

Chen, C. M. 1998 *Modeling Drinking Water Disinfection in Ozone Bubble-Diffuser Contactors*. PhD thesis, Purdue University, West Lafayette, Indiana.

Clift, R., Grace, J. R. & Weber, M. E. 1978 *Bubbles, Drops and Particles*. Academic Press, New York.

Cockx, A., Liné, A., Roustan, M., Do-Quang, Z. & Lazarova, V. 1997 Numerical simulation and physical modeling of the hydrodynamics in an air-lift internal loop reactor. *Chem. Eng. Sci.* **52**(21-22), 3787–3793.

Cockx, A., Do-quang, Z., Line, A. & Roustan, M. 1999 Use of computational fluid dynamics for simulating hydrodynamics and mass transfer in industrial ozonation towers. *Chem. Eng. Sci.* **54**(21), 5085–5090.

Danckwerts, P. V. 1970 *Gas-Liquid Reactions*. McGraw-Hill, New York.

Do-Quang, Z., Cockx, A., Liné, A. & Roustan, M. 1999 Computational fluid dynamics applied to water and wastewater treatment facility modeling. *Environ. Eng. Pol.* **1**(3), 137–147.

El-Baz, G. 2002 *Développement d'un modèle de calcul de la performance des unités de désinfection*. MASc thesis, École Polytechnique de Montréal, Montréal, Québec, Canada.

Gobby, G. 2004 *Experimental Validation of a Bubble Column Reactor*. CFX validation report (CFX-VAL08/0404), Ansys Inc., Canonsburg, PA. USA.

Hunt, N. K. & Marinas, B. J. 1999 Inactivation of *Escherichia coli* with ozone: chemical and inactivation kinetics. *Wat. Res.* **33**(11), 2633–2641.

Kim, J. H., Rennecker, J. L., Tomiakm, R. B., Mariñas, B. J., Miltner, R. J. & Owens, J. H. 2002 Inactivation of *Cryptosporidium oocysts* in a pilot-scale bubble-diffuser contactor II: Model validation and application. *J. Environ. Eng.-ASCE* **128**(6), 522–532.

Lakehal, D. 2002 Modeling of multiphase turbulent flows for environmental and hydrodynamic applications. *Int. J. Multiphase Flow* **28**(5), 823–863.

Langlais, B., Reckhow, D. A. & Brink, D. R. 1991 *Ozone in Water Treatment: Application and Engineering*. Lewis Publisher, Chelsea, Michigan.

Launder, B. & Spalding, D. 1974 The numerical computation of turbulent flows. *Comp. Meth. Appl. Mech. Eng.* **3**, 269–289.

Lev, O. & Regli, S. 1992 Evaluation of ozone disinfection systems: Characteristic concentration-C. *J. Environ. Eng.-ASCE* **118**(4), 477–494.

Levenspiel, O. 1999 *Chemical Reaction Engineering, 2nd edn*. John Wiley and Sons, New York.

Lo, M. 2000 Application of population balance to CFD modelling of gas-liquid reactors. *Proceedings of Conference on Trends in Numerical and Physical Modelling for Industrial Multiphase Flows Conference*, 27–29 September, Corse, France.

Lopez de Bertodano, B. 1991 *Turbulent Bubbly Flow in a Triangular Duct*. PhD thesis, Rensselaer Polytechnic Institute, Troy, New York.

Marinas, B. J., Liang, S. & Aieta, E. M. 1993 Modeling hydrodynamics and ozone residual distribution in a pilot-scale ozone bubble-diffuser contactor. *J. Am. Wat. Wks Assoc.* **85**(3), 90–99.

Menter, F. R. 1994 Two-equation eddy-viscosity turbulence models for engineering application. *J. Am. Inst. Aeronaut. Astronaut.* **32**(8), 1598–1605.

MENV (Ministère de l'environnement du Québec) 2002 *Guide de conception des installations de production d'eau potable*, www.mddep.gouv.qc.ca/eau/potable/guide/index.htm.

Michele, V. 2002 CFD *modeling and measurement of liquid flow structure and phase holdup in two-and three-phase bubble columns*. PhD dissertation, University of Braunschweig, Germany.

MOE (Ontario Ministry of Environment) 2006 *Procedure for disinfection of drinking water in Ontario*, www.ene.gov.on.ca/envision/gp/4448e01.pdf.

Murrer, E. W., Gunstead, J. & Lo, S. 1995 The Development of an ozone contact tank simulation model. *Proceedings of the 12th World Congress of the International Ozone Association*, 15–18 May 1995, Lille, France.

Peplinski, D. K. & Ducoste, J. J. 2002 Modelling of disinfection contactor hydraulics under uncertainty. *J. Environ. Eng.* **11**, 1056–1067.

Rakness, K. L. 2005 *Ozone in Drinking Water Treatment: Process Design, Operation and Optimization*. American Water Works Association, Denver, Colorado.

Roustan, M., Line, A. & Wable, O. 1992 Modeling of vertical downward gas-liquid flow for the design of a new contactor. *Chem. Eng. Sci.* **47**(13-14), 3681–3688.

Sato, Y. & Sekoguchi, K. 1975 Liquid velocity distribution in two-phase bubble flow. *Int. J. Multiphase Flow* **2**, 79–95.

Schugerl, K. & Bellgardt, K. H. 2001 *Bioreaction Engineering: Modeling and Control*. Springer, Berlin.

Singer, P. C. & Hull, C. S. 2000 *Modeling Dissolved Ozone Behaviour in Ozone Contactors*. Report No. 90769, American Water Works Association, Research Foundation, Denver, Colorado.

Speziale, C. G., Sarkar, S. & Gatski, T. B. 1991 Modeling the pressure-strain correlation of turbulence: an invariant dynamical system approach. *J. Fluid Mech.* **227**, 245–272.

*Standard Methods for the Examination of Water and Wastewater* 1998 20th edition, American Public Health Association/American Water Works Association/Water Environment Federation, Washington, DC.

Ta, C. & Hague, J. 2004 A two-phase computational fluid dynamics model for ozone tank design and troubleshooting in water treatment. *Ozone: Sci. Eng.* **26**(4), 403–411.

Tang, G., Adu-Sarkodie, K., Kim, D., Kim, J. H., Teefy, S., Shukairy, H. M. & Marinas, B. J. 2005 Modeling *Cryptosporidium parvum* oocyst inactivation and bromate formation in a full-scale ozone contactor. *Environ. Sci. Technol.* **39**(23), 9343–9350.

Teefy, S. 1996 *Tracer Studies in Water Treatment Facilities*. Report No. 90692, American Water Works Association, Research Foundation, Denver, Colorado.

USEPA 1991 *Surface Water Treatment Rule Guidance Manual*. US Environmental Protection Agency, Washington, DC.

USEPA 2006 *Long Term 2 Surface Water Treatment Rule (LT2 SWTR Rule)*. US Environmental Protection Agency, Washington, DC.

Versteeg, H. K. & Malalasekera, W. 2002 *An Introduction to Computational Fluid Dynamics: The Finite Volume Method*. Addison-Wesley, Harlow, UK.

Vesvikar, M. S. & Al-Dahhan, M. 2005 Flow pattern visualization in a mimic anaerobic digester using CFD. *Biotechnol. Bioeng.* **89**(6), 719–732.

Yakhot, V. & Orzag, S. A. 1986 Renormalization group analysis of turbulence: basic theory. *J. Sci. Comput.* **1**(1), 1–51.

Zhang, J. 2007 *An Integrated Design Approach for Improving Drinking Water Ozone Disinfection Treatment Based on Computational Fluid Dynamics*. PhD thesis, University of Waterloo, Canada.

Zhang, J., Anderson, W. B., Smith, E. F., Barbeau, B., Desjardins, R. & Huck, P. M. 2005 Development, validation and implementation of a multiphase CFD model for optimization of full-scale ozone disinfection processes. *Proceedings of the American Water Works Association Water Quality Technology Conference and Exposition (WQTC)*, 6–10 November 2005, Quebec City, Quebec.

Zhou, H., Smith, D. W. & Stanley, S. J. 1994 Modeling of dissolved ozone concentration profiles in bubble columns. *J. Environ. Eng. ASCE* **120**(4), 821–840.

First received 1 April 2007; accepted in revised form 19 September 2007

## APPENDIX 1 SENSITIVITY TO MESH DENSITY

As the mesh is refined a more accurate solution can be expected; however, the finer the mesh, the more time is needed for computations. Therefore, the mesh density should be selected such that an acceptably accurate solution is obtained within a reasonable simulation time. At the same time, it is necessary that the solution obtained is mesh-independent (Vesvikar & Al-Dahhan 2005). In this study, the effect of mesh density on the accuracy of CFD modelling was evaluated by performing a series of tracer residence time distribution simulations at three different mesh density conditions. The number of elements for the three meshes was 320,803, 370,982 and 424,891, respectively. Figure 11 presents the comparison result which suggests that there was only a slight difference in tracer RTD prediction under the three mesh density conditions. T10, T50 and T90 values, the times for 10%, 50% and 90% of tracer to pass through the contactor exit, respectively, were calculated from the tracer simulation results. It was found that the maximum percentage difference in predicted T10, T50 and T90 from the finest and medium meshes were 5.7%, 1.5% and 2.4%, respectively. Further reduction of mesh size did not significantly improve the accuracy of modelling. To ensure the quality of the mesh, a mesh size of 424,891 was selected for the rest of the studies.

## APPENDIX 2 SENSITIVITY TO CHOICE OF TURBULENCE MODEL

The effect of the turbulence model on the tracer RTD was also studied. In addition to the standard k–ϵ model, three other commonly used turbulence models including the RNG k–εmodel (Yakhot & Orzag 1986), the shear stress transport (SST) turbulence model (Menter 1994) and the Speziale-Sarkar-Gatski (SSG) model (Speziale *et al.* 1991) were used for comparison purposes. Figure 12 shows tracer RTD simulation results for the different models. In all four cases the tracer curves varied slightly and the standard k–ε model fit best with the experimental results. This suggested that the k–ϵ model was most appropriate for the study undertaken here. In addition, the RNG k–ϵ, SST and SSG models usually require much longer computational times. Therefore, the k–ϵ model was selected for this study.

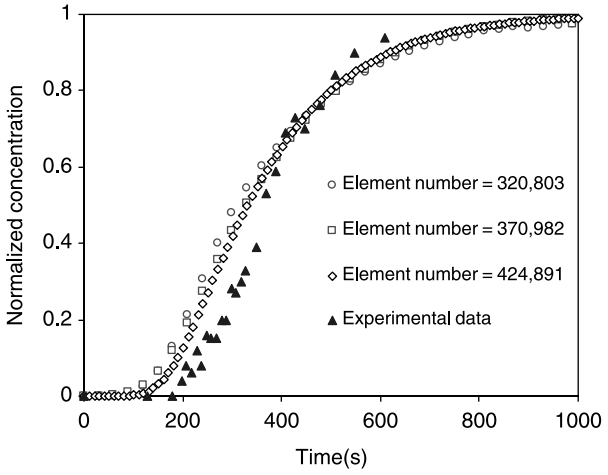


**Figure 11** | Impact of the mesh density on the simulation of tracer residence time distribution.

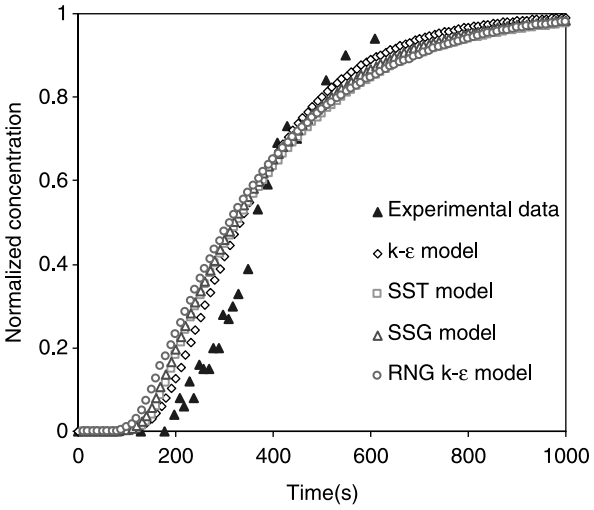


**Figure 12** | Impact of the turbulence model on the simulation of tracer residence time distribution.